Am J Physiol Heart Circ Physiol 298: H24–H32, 2010.
First published October 16, 2009; doi:10.1152/ajpheart.00799.2009.

Direct evidence of a role for Nox2 in superoxide production, reduced nitric oxide bioavailability, and early atherosclerotic plaque formation in ApoE$^{-/-}$ mice

Courtney P. Judkins,[1]* Henry Diep,* Brad R. S. Broughton,[1] Anja E. Mast,[1] Elizabeth U. Hooker,[1] Alyson A. Miller,[1] Stavros Selemidis,[1] Gregory J. Dusting,[2] Christopher G. Sobey,[1] and Grant R. Drummond[1]

[1]*Department of Pharmacology, Monash University, Clayton, Victoria, and* [2]*Bernard O'Brien Institute of Microsurgery, University of Melbourne, Fitzroy, Australia*

Submitted 24 August 2009; accepted in final form 13 October 2009

Judkins CP, Diep H, Broughton BR, Mast AE, Hooker EU, Miller AA, Selemidis S, Dusting GJ, Sobey CG, Drummond GR. Direct evidence of a role for Nox2 in superoxide production, reduced nitric oxide bioavailability, and early atherosclerotic plaque formation in ApoE$^{-/-}$ mice. *Am J Physiol Heart Circ Physiol* 298: H24–H32, 2010. First published October 16, 2009; doi:10.1152/ajpheart.00799.2009.—The Nox family NADPH oxidases are reactive oxygen species (ROS)-generating enzymes that are strongly implicated in atherogenesis. However, no studies have examined which Nox isoform(s) are involved. Here we investigated the role of the Nox2-containing NADPH oxidase in atherogenesis in apolipoprotein E-null (ApoE$^{-/-}$) mice. Wild-type (C57Bl6/J), ApoE$^{-/-}$, and Nox2$^{-/y}$/ApoE$^{-/-}$ mice were maintained on a high-fat (21%) diet from 5 wk of age until they were 12 or 19 wk old. Mice were euthanized and their aortas removed for measurement of Nox2 expression (Western blot analysis and immunohistochemistry), ROS production (L012-enhanced chemiluminescence), nitric oxide (NO) bioavailability (contractions to N^{ω}-nitro-L-arginine), and atherosclerotic plaque development along the aorta and in the aortic sinus. Nox2 expression was upregulated in the aortic endothelium of ApoE$^{-/-}$ mice before the appearance of lesions, and this was associated with elevated ROS levels. Within developing plaques, macrophages were also a prominent source of Nox2. The absence of Nox2 in Nox2$^{-/y}$/ApoE$^{-/-}$ double-knockout mice had minimal effects on plasma lipids or lesion development in the aortic sinus in animals up to 19 wk of age. However, an en face examination of the aorta from the arch to the iliac bifurcation revealed a 50% reduction in lesion area in Nox2$^{-/y}$/ApoE$^{-/-}$ versus ApoE$^{-/-}$ mice, and this was associated with a marked decrease in aortic ROS production and an increased NO bioavailability. In conclusion, this is the first demonstration of a role for Nox2-NADPH oxidase in vascular ROS production, reduced NO bioavailability, and early lesion development in ApoE$^{-/-}$ mice, highlighting this Nox isoform as a potential target for future therapies for atherosclerosis.

Nox isoforms; reactive oxygen species; endothelial dysfunction

ELEVATED VASCULAR reactive oxygen species (ROS) production is postulated to be an early triggering mechanism for atherosclerosis by causing oxidative stress, activation of proinflammatory signaling cascades, and breakdown of vasoprotective nitric oxide (NO). Clinical trials assessing the effects of antioxidants (i.e., ROS scavengers) on cardiovascular events and the progression of atherosclerosis have been overwhelmingly disappointing (8). Thus the identification of the sources of ROS in atherogenesis may pave the way for alternative therapies that combat vascular oxidative stress by blocking ROS production from the outset.

The Nox-containing NADPH oxidases are a family of enzymes for which the only ascribed function is the generation of ROS (4, 25). NADPH oxidases comprise a membrane-bound catalytic subunit that transfers electrons from NADPH to molecular oxygen (Nox1-5), a smaller membrane-bound protein that stabilizes the Nox subunit within membranes (p22^{phox}), and up to three cytosolic regulatory subunits including an organizer protein (p47^{phox} or Noxo1), an activator protein (p67^{phox} or Noxa1), and a small GTPase (Rac1 or Rac2) (21, 25). At least three isoforms of NADPH oxidase are expressed in the blood vessel wall, differing from one another in both the Nox homolog they utilize and in their reliance on specific regulatory subunits (9, 25). These include a Nox4-containing isoform, which is expressed at high levels under physiological conditions in all of the constitutive cell types of the blood vessel wall (i.e., endothelial cells, vascular smooth muscle cells, and adventitial fibroblasts) and the activity of which probably relies only on its association with p22^{phox} (1, 18). Unlike Nox4, the two remaining isoforms, Nox1 and Nox2, are expressed at low levels in the vasculature during physiology but are upregulated in cardiovascular risk settings including hypertension, diabetes, and hyperlipidemia (5, 19, 29). Nox1- and Nox2-containing NADPH oxidases display a restricted pattern of localization compared with Nox4-NADPH oxidases, with Nox2 being expressed in endothelial cells and adventitial fibroblasts and invading inflammatory cells of developing atherosclerotic lesions and with Nox1 being confined to vascular smooth muscle cells and possibly endothelial cells (26). Moreover, the activity of Nox1 and Nox2 in vascular cells is reliant on association with not only p22^{phox} but also p47^{phox}, which acts as a chaperone for the activator protein (p67^{phox} or Noxa1) and Rac1 (2).

Apolipoprotein E-null (ApoE$^{-/-}$) mice are the most widely studied animal model of atherosclerosis. These mice are hypercholesterolemic and spontaneously develop atherosclerotic plaques in the aorta and arterial branches thereof. Three previous studies have directly investigated the role of NADPH oxidases in atherogenesis in ApoE$^{-/-}$ mice through the genetic deletion of p47^{phox} (i.e., via generation of p47$^{phox-/-}$/ApoE$^{-/-}$ double knockouts) (3, 14, 28). These studies indicated that, although p47^{phox} expression may not contribute to lesion development in the aortic sinus of ApoE$^{-/-}$ mice, it plays a major role in atherogenesis in the descending aorta, with the

* C. P. Judkins and H. Diep contributed equally to this work.

Address for reprint requests and other correspondence: G. R. Drummond, Dept. of Pharmacology, Monash Univ., Bldg. 13E, Wellington Rd., Clayton, Victoria 3800, Australia (e-mail: grant.drummond@med.monash.edu.au).

deletion of $p47^{phox}$ resulting in up to an 80% smaller lesion area.

The above studies provide no insight into which of the $p47^{phox}$-dependent NADPH oxidase isoforms in the vasculature, Nox1 versus Nox2, are involved in atherogenesis in mice. Indeed, only one previous study investigated this directly; however, in that study, the effect of Nox2 deletion on atherosclerosis was only examined via its impact on intimal thickening in the aortic sinus where it was found to have no role in animals up to 24 wk of age (15). This finding was perhaps not surprising in light of the reports that $p47^{phox}$ also had no effect on lesion size in the aortic sinus (3, 14). Therefore, we hypothesized that, like $p47^{phox}$, Nox2-dependent NADPH oxidase activity plays little role in atherogenesis in the aortic sinus of $ApoE^{-/-}$ mice but is a significant contributor to plaque development along the length of the aorta. To test this hypothesis, we generated genetically related strains of $Nox2^{-/y}/ApoE^{-/-}$ double-knockout and $ApoE^{-/-}$ single-knockout mice and compared vascular ROS production, NO bioavailability, and atherosclerotic plaque formation in both the aortic sinus and along the ascending and descending segments of the aorta. As reported previously (15), we found no differences in plaque development in the aortic sinus between $Nox2^{-/y}/ApoE^{-/-}$ and $ApoE^{-/-}$ mice. However, Nox2 deletion was associated with a profound reduction in superoxide production, a significant improvement in NO bioavailability, and markedly less atherosclerotic plaque burden along the length of the aorta. Hence, these studies are the first to provide a direct cause and effect evidence for a specific NADPH oxidase isoform, namely, Nox2, in early atherogenesis in mice.

METHODS

Experimental Animals

$Nox2^{-/-}$ (also known as $gp91^{phox-/-}$) mice were originally generated in the laboratory of Prof. Mary Dinauer (22) and bred at Ozgene (Australia). $ApoE^{-/-}$ and wild-type mice were obtained from the Animal Resource Centre (Australia). All mice were fully backcrossed to the C57BL/6J background. Female $Nox2^{+/-}/ApoE^{+/+}$ mice were crossed with male $Nox2^{+/y}/ApoE^{-/-}$ mice to produce an F1 generation. From this F1 generation, female $Nox2^{+/-}/ApoE^{+/-}$ mice were crossed with males of either the $Nox2^{+/y}/ApoE^{+/-}$ or $Nox2^{-/y}/ApoE^{+/-}$ genotype. The resulting F2 generation consisted of male and female wild-type ($Nox2^{+/y}/ApoE^{+/+}$ and $Nox2^{+/+}/ApoE^{+/+}$), $ApoE^{-/-}$ ($Nox2^{+/y}/ApoE^{-/-}$ and $Nox2^{+/+}/ApoE^{-/-}$), and double-knockout ($Nox2^{-/y}/ApoE^{-/-}$and $Nox2^{-/-}/ApoE^{-/-}$) mice. Males and females of each genotype were set up as homozygous breeding pairs to generate an F3 generation of genetically related strains of wild-type, $ApoE^{-/-}$, and $Nox2^{-/y}/ApoE^{-/-}$ mice that were ultimately used for experiments. Genotypes were determined by PCR amplification of tail DNA.

Male mice were weaned at 3 wk of age, maintained on a 12-h:12-h dark-light cycle (23 ± 2°C), and given access to standard rodent chow and water ad libitum. From 5 wk of age, the mice were placed on a Western-style diet (21% fat and 0.15% cholesterol; SFOO-219, Specialty Feeds) and maintained on this until they were 12 or 19 wk of age. The 12-wk age group was chosen because it represented a time point at which atherosclerotic plaque burden along the aorta was minimal, thus allowing us to determine whether changes in Nox2 activity and expression were evident from early in the disease process. The 19-wk time point was chosen since it was comparable with an earlier study in $p47^{phox-/-}/ApoE^{-/-}$ mice (3, 14), which provided important background information for the present study. Once mice reached appropriate ages, they were heparinized (500 IU ip; DBL) and anesthetized with isoflurane (Baxter Healthcare) before being euthanized by decapitation.

All procedures were approved by the Monash University School of Biomedical Sciences Animal Ethics Committee.

Plasma Lipid Profile Analysis

Blood was obtained from the abdominal vena cava, and plasma was isolated by centrifugation (4,000 *g*, 4°C, 10 min). Plasma concentrations of total cholesterol, high-density lipoprotein (HDL) cholesterol, and triglycerides were determined using Roche CHOL, HDL-cholesterol plus, and triglyceride assays, respectively (Roche). Low-density lipoprotein (LDL) cholesterol was calculated as the difference between total- and HDL-cholesterol concentrations.

Assessment of Atherosclerotic Lesions

Atherosclerotic lesion burden was quantified along the luminal surface of the aorta and through serial sections of the aortic sinus (3, 14, 15). For the former, aortas were dissected out in their entirety from just distal (~1 mm) to the coronary sinus to just proximal (~1 mm) to the iliac bifurcation. Aortas were then cut open longitudinally along the ventral surface and incubated for 30 min with oil red O (0.5% in 60% isopropyl alcohol). Excess stain was removed with 60% isopropyl alcohol, and en face images of each aortic segment were photographed. The atherosclerotic plaque area was expressed as a percentage of the total luminal surface area of the aorta.

Aortic sinuses were cut into 10-μm sections, thaw mounted onto poly-L-lysine-coated microscope slides, and stained with oil red O solution (0.03% in 60% isopropyl alcohol) for 30 min. The sections were then counterstained with hematoxylin. The sections were photographed using an Olympus BX51 microscope (Olympus), and the intimal and medial areas were then quantified using Motic Images 2000 software (Motic China Group). Atherosclerotic plaque size in the aortic sinus was expressed as an intima-to-media ratio (IMR).

ROS Detection

Basal ROS production in segments of mouse aorta was assessed by L012-enhanced chemiluminescence (11, 12). The aortas were dissected out in their entirety as described in *Assessment of Atherosclerotic Lesions*, before being cut into 10 ring segments of 2 to 3 mm in length. On average, we obtained two rings from the arch, five rings from the thoracic, and three rings from the abdominal regions of the aorta. Each aortic ring was placed in separate wells of a white 96-well plate containing Krebs-HEPES solution. The rings were allowed to equilibrate for 30 min at 37°C before the addition of L012 (100 μmol/l; Wako Pure Chemical Industries). L012-enhanced chemiluminescence was then measured every 2 min over a 50-min period using a Plate Chameleon Luminescence Reader (Hidex). L012 chemiluminescence was also measured in adjacent wells devoid of tissue (blanks). Superoxide production by each ring segment was calculated by subtracting the chemiluminescence signal (relative light units per s) obtained in the blank wells from the signal detected in the well containing that ring and then normalized to dry tissue weight (in mg). For each animal, the data points thus represent the average tissue-dependent chemiluminescence detected from 10 separate rings representing the entire length of the aorta.

In pilot experiments, we demonstrated that the L012-chemiluminescence signal detected from aortic rings of wild-type mice is abolished by superoxide dismutase (300 U/ml) and Tempol (10 mmol/l) but not affected by ebselen (30 μmol/l), implying that it is due to superoxide and not other ROS such as hydrogen peroxide and peroxynitrite (supplemental Fig. 1; note: all supplemental material may be found posted with the online version of this article).

Western Blot Analysis

Aortas were dissected out in their entirety from just distal to the coronary sinus to just proximal to the iliac bifurcation, snap frozen in

liquid nitrogen, pulverized, and homogenized by the addition of Laemmli buffer [containing 5% glycerine, 2.5% mercaptoethanol, 1.5% SDS, 50 mmol/l Tris·HCl (pH 8.0), 0.05 mg/ml Bromophenol blue] and subsequent sonification. Samples were heated to 37°C for 10 min, and 40 μg of protein (determined by RCDC kit; Bio-Rad) were separated by SDS-PAGE (7.5% acrylamide:bis acrylamide) and transferred to Immobilon-P polyvinylidene difluoride membrane (Millipore) by semidry blotting at 2 mA/cm^2 for 1 h. The membranes were blocked for 1 h in Tris-buffered saline containing 3% skim milk and incubated overnight (4°C) with either mouse anti-Nox2 monoclonal (1:1,000; BD Biosciences) or rabbit anti-Nox4 polyclonal (1:1,000; Abcam) primary antibodies. Membranes were washed with Tris-buffered saline, incubated for 1 h with goat anti-mouse or goat anti-rabbit secondary antibodies (1:10,000; Jackson Immuno Research), and then exposed to enhanced chemiluminescence reagents (GE Healthcare). Bands were visualized using X-ray film. An anti-GAPDH monoclonal antibody (1:10,000; AbCAM) was used to normalize for loading variations.

Immunohistochemistry

Aortas were dissected out in their entirety from just distal to the coronary sinus to just proximal to the iliac bifurcation, before being divided into arch, thoracic (for immunohistochemistry studies), and abdominal (for vascular reactivity studies) sections. For immunohistochemistry studies, thoracic aortas were frozen in optimum cutting temperature compound, sectioned at 10 μm, and thaw mounted onto gelatinized slides. Following a fixation in acetone, the sections were incubated overnight with a mouse monoclonal anti-Nox2 antibody (1:1,000, BD Biosciences) and rabbit polyclonal antibodies against either von Willebrand factor (vWF, 1:1,000, AbCAM), smooth muscle actin (1:50, AbCAM), CD3 (1:50, AbCAM), or CD68 (1:50, Santa Cruz). The sections were then washed in phosphate-buffered saline (PBS) and incubated in fluorescein isothiocyanate-conjugated goat anti-mouse IgG (1:200, Zymed) and Texas red-labeled goat anti-rabbit IgG (1:200, Zymed) antibodies for 4 h. The sections were again washed in PBS and photographed with a Leica TCS NT confocal microscope (Leica).

Contractile Responses of Isolated Aortic Rings to N$^{\omega}$-Nitro-L-Arginine Methyl Ester

Contractile responses to N^{ω}-nitro-L-arginine methyl ester (L-NAME), as an indicator of NO bioavailability, were measured in rings of abdominal aorta isolated from ApoE$^{-/-}$ and Nox2$^{-/y}$/ApoE$^{-/-}$ mice. Our choice of abdominal ring segments in these studies was based on preliminary observations in our laboratory that this region of the mouse aorta is resistant to the development of phasic contractile activity (data not shown). This is in stark contrast to rings derived from the arch and thoracic regions of the aorta which display marked oscillations in tone in the presence of the precontraction agent U-46619. Abdominal aortic rings were mounted on stainless steel wires between an isometric force transducer and a micrometer in the organ chamber of a Mulvany-Halpern myograph filled with carbogen-bubbled Krebs-bicarbonate solution. After a 20-min equilibration at 37°C, the rings were stretched to a resting tension of 5 mN and then maximally contracted with a bolus concentration of U-46619 (0.3 μmol/l). Subsequently, the rings were washed with fresh Krebs and allowed to return to resting levels of tension before being precontracted to 20% of their respective maximum contraction with titrated concentrations of U-46619. Finally, L-NAME (100 μmol/l) was added and the contractile response was recorded until it reached a plateau.

Statistical Analysis

Data are presented as means ± SE. Data were analyzed using Student's unpaired *t*-test to detect a statistical difference between the group of interest and its control, i.e., between ApoE$^{-/-}$ and age-matched wild-type mice or between Nox2$^{-/y}$/ApoE$^{-/-}$ and age-matched ApoE$^{-/-}$ mice. $P < 0.05$ was considered significant.

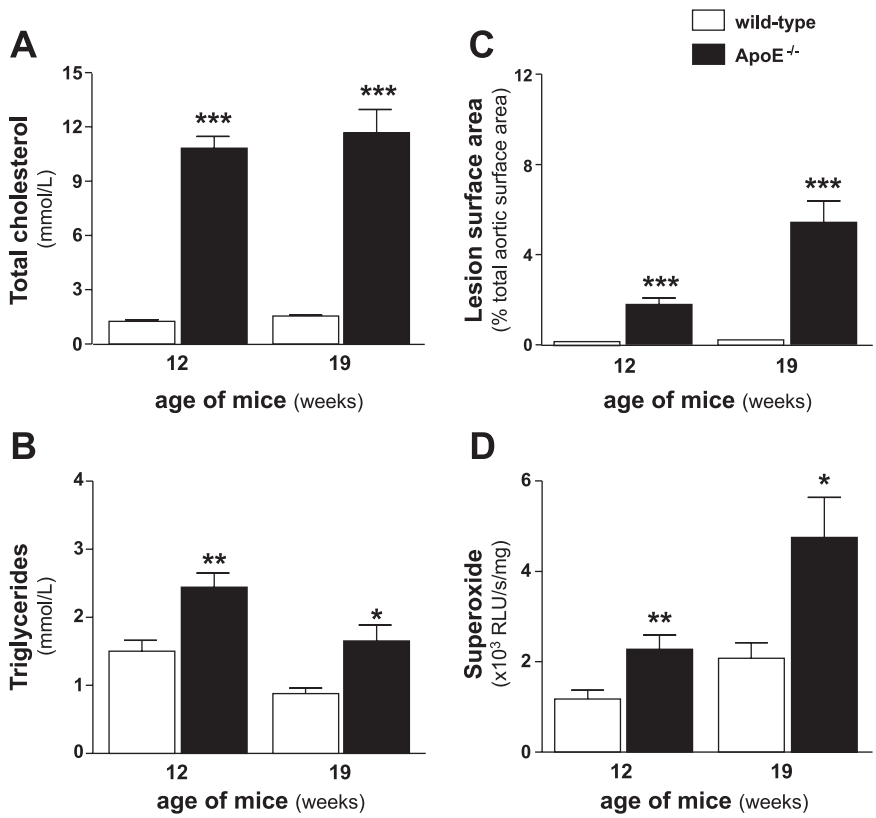

Fig. 1. Hypercholesterolemia and atherosclerosis in apolipoprotein E-null (ApoE$^{-/-}$) mice are associated with elevated vascular reactive oxygen species production. Total plasma cholesterol (*A*) and triglycerides (*B*) and aortic en face atherosclerotic lesion coverage (*C*) in wild-type (WT) and ApoE$^{-/-}$ mice maintained on a Western-style diet from 5 wk of age are shown. *D*: superoxide levels measured by L012-enhanced chemiluminescence and expressed as relative luminescence units (RLU) per second per mg of tissue weight in isolated aortic ring segments from WT and ApoE$^{-/-}$ mice. *$P < 0.05$, **$P < 0.01$, and ***$P < 0.001$ vs. age-matched WT mice ($n \geq 5$).

RESULTS

Hypercholesterolemia and Atherosclerosis in ApoE$^{-/-}$ Mice Are Associated with Elevated Vascular ROS Production and Nox2 Expression

Plasma lipid profiles. Total cholesterol levels were substantially higher in ApoE$^{-/-}$ than in wild-type mice at 12 (8.6-fold; $P < 0.001$) and 19 (7.5-fold; $P < 0.001$) wk of age (Fig. 1*A*). These increases in total cholesterol resulted from marked increases in levels of circulating LDL cholesterol at 12 (65-fold; $P < 0.001$) and 19 (39-fold; $P < 0.001$) wk of age and relatively modest increases in levels of HDL cholesterol at 12 (2.8-fold; $P < 0.001$) and 19 (2.5-fold; $P < 0.001$) wk of age (supplemental Fig. 2). Plasma triglyceride levels were also elevated by approximately twofold in ApoE$^{-/-}$ versus wild-type mice in both of the age groups studied (Fig. 1*B*).

Atherosclerotic lesion burden. Lesion coverage of the aorta was minimal (i.e., 1.8 ± 0.2%) in ApoE$^{-/-}$ mice at 12 wk of age (Fig. 1*C*). An examination of the separate sections of the aorta from these 12-wk-old mice revealed that the majority of the lesions that were present occurred in the arch, with few lesions evident in the thoracic and abdominal sections (supplemental Fig. 3). By 19 wk of age, the lesion coverage along the aorta increased to 5.5 ± 1.0% (Fig. 1*C*). At this age, the plaques were now prominent in both the arch and abdominal sections, with the thoracic sections still largely devoid of lesions (supplemental Fig. 3). By contrast, no atherosclerotic lesions were observed in wild-type mice maintained on a Western diet at either of the ages studied (Fig. 1*C*, and supplement Fig. 3).

ROS production. Despite minimal lesion burden in 12-wk-old ApoE$^{-/-}$ mice, aortic ROS levels were already elevated by approximately twofold compared with age-matched wild-type mice (Fig. 1*D*). Aortic ROS levels remained elevated in ApoE$^{-/-}$ versus wild-type mice at 19 wk of age (Fig. 1*D*).

Nox2 and Nox4 protein expression. In the present study, we used spleen homogenates from wild-type and Nox2$^{-/-}$ mice as positive and negative controls, respectively, for Nox2 and demonstrated that the protein runs as a single band at 58 kDa on SDS-PAGE (Fig. 2), as reported previously (7). The expression of Nox2 (58 kDa) was 3.8-fold higher ($P < 0.001$) in aortic homogenates from 12-wk-old ApoE$^{-/-}$ mice than in age-matched wild-types (Fig. 2*A*). Nox2 (58 kDa) expression remained elevated in aortas from ApoE$^{-/-}$ versus wild-type mice at 19 wk of age (Fig. 2*A*). Interestingly, at this later age, additional bands with higher apparent molecular masses of ~65, ~90, and ~110 kDa were detected in aortic homogenates from ApoE$^{-/-}$ mice and, to a lesser extent, in the wild-type tissues (Fig. 2*A*).

In contrast to Nox2, a 70-kDa immunoreactive band detected with an anti-Nox4 antibody was unchanged in ApoE$^{-/-}$ versus wild-type mice at both 12 and 19 wk of age (Fig. 2*B*).

Nox2 localization. Arterial sections from 19-wk-old wild-type mice were weakly immunoreactive for Nox2, with the majority of Nox2 immunofluorescence observed in the intimal layer, colocalized with the endothelial cell marker vWF (Fig. 3*A*). In arterial sections from 19-wk-old ApoE$^{-/-}$ mice that were free of atherosclerotic lesions, Nox2 immunofluorescence was substantially more intense than that observed in wild-types (Fig. 3*B*). Again, Nox2 was predominantly expressed in the intima, colocalized with vWF. Nox2 also appeared to be expressed in the adventitial layer of these lesion-free sections from ApoE$^{-/-}$ mice (Fig. 3*B*). Finally, Nox2 was absent from the medial layer of the arterial sections from

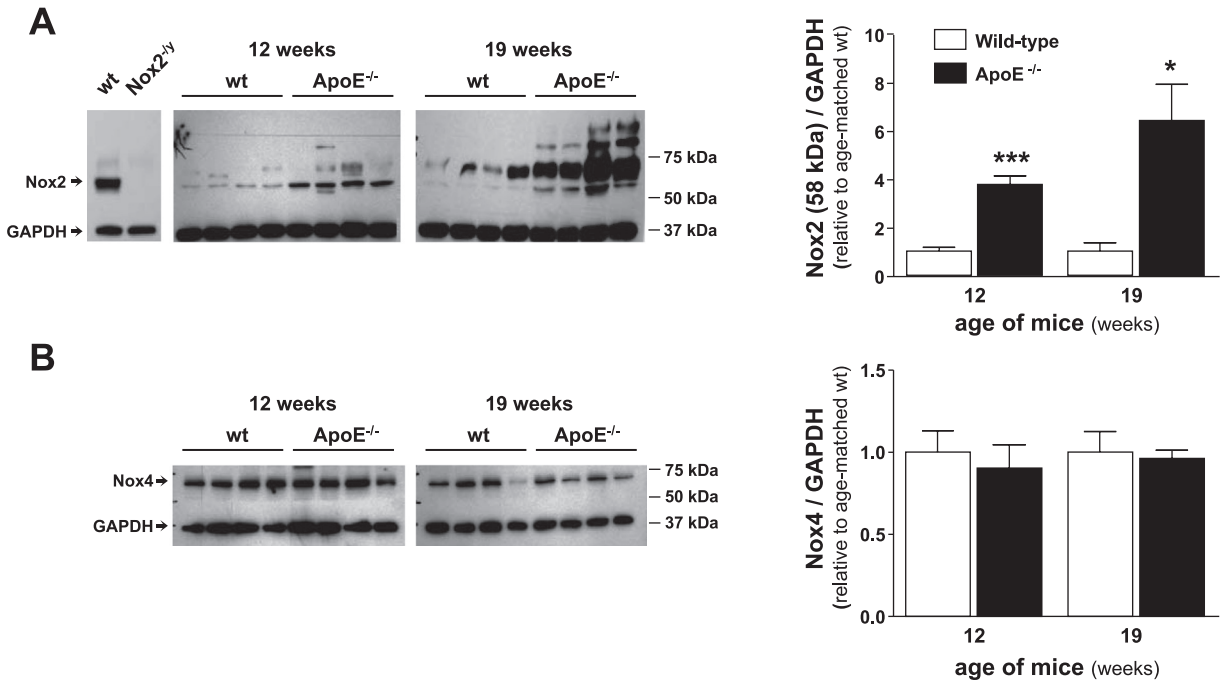

Fig. 2. Upregulation of Nox2 but not Nox4 protein expression in aortas from ApoE$^{-/-}$ mice. Western blot images (*left*) and grouped densitometric data (*right*) show protein expression of Nox2 (*A*) and Nox4 (*B*) in whole aortic homogenates from WT and ApoE$^{-/-}$ mice maintained on a Western-style diet from 5 wk of age. In *A*, *far left*: immunoreactive bands detected by the anti-Nox2 antibody in spleen homogenates from WT (positive control) and Nox2$^{-/y}$ (negative control) mice. *$P < 0.05$ and ***$P < 0.001$ vs. age-matched WT mice ($n = 4$).

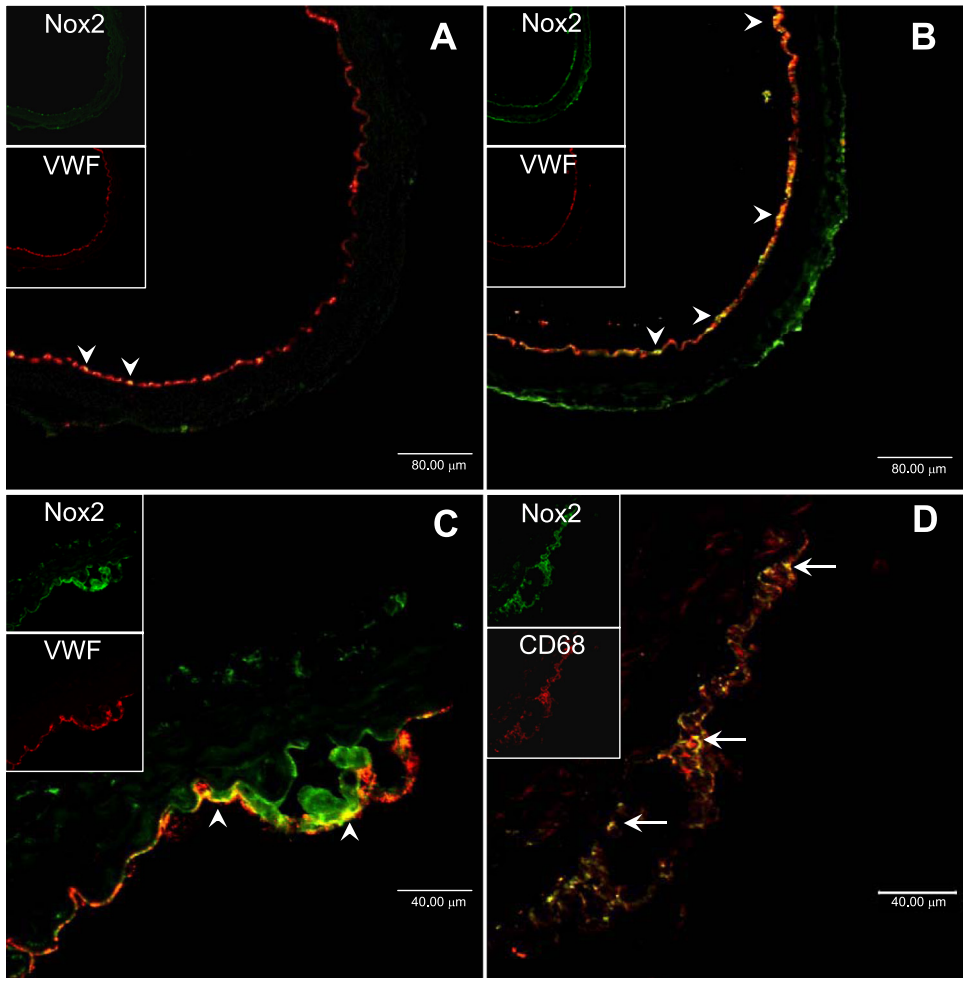

Fig. 3. Localization of Nox2 to aortic endothelial cells and macrophages in ApoE$^{-/-}$ mice. Representative photomicrographs show cellular localization of Nox2 in aortas from 19-wk-old WT (*A*) and ApoE$^{-/-}$ (*B–D*) mice maintained on a Western-style diet from 5 wk of age. Nox2 immunoreactivity is shown in green, whereas immunoreactivity for the endothelial cell [von Willebrand factor (vWF)]- and macrophage (CD68)-specific markers are shown in red. Colocalization of Nox2 with vWF and CD68 is shown in yellow and highlighted by arrowheads and arrows, respectively. Scale bars are 80 μm (*A* and *B*) and 40 μm (*C* and *D*).

ApoE$^{-/-}$ mice, and we could find no evidence of colocalization with the smooth muscle-specific marker α-smooth muscle actin (data not shown).

We also examined Nox2 immunoreactivity in arterial sections from 19-wk-old ApoE$^{-/-}$ mice that contained atherosclerotic lesions. Nox2 immunoreactivity was observed throughout the plaque but was most intense at the plaque shoulder (Fig. 3*C*). Again, Nox2 immunofluorescence was colocalized with the endothelial cell marker vWF (Fig. 3*C*). Nox2 immunofluorescence was additionally observed to be colocalized with CD68, a macrophage-specific marker (Fig. 3*D*), but not with smooth muscle (α-actin) or T-cell (CD3) markers (data not shown).

Effect of Nox2 Deletion on Plasma Lipid Profiles and Atherosclerotic Plaque Development in ApoE$^{-/-}$ Mice

Given our findings of elevated Nox2 expression in the vascular wall of ApoE$^{-/-}$ mice, we next examined for a cause and effect relationship between this isoform of NADPH oxidase and atherogenesis by generating a colony of Nox2$^{-/y}$/ApoE$^{-/-}$ mice and comparing the disease progression in these animals with that in a colony of ApoE$^{-/-}$ mice bred from F3 generation siblings. The absence of Nox2 in mice from the double-knockout colony was confirmed by PCR genotyping (data not shown), as well as by immunofluorescence in a subset of animals (Fig. 4). Plasma lipid profiles were only marginally different between the Nox2$^{-/y}$/ApoE$^{-/-}$ and ApoE$^{-/-}$ strains. At 12 wk of age, total cholesterol was slightly lower (by 15%; $P < 0.05$) in Nox2$^{-/y}$/ApoE$^{-/-}$ versus ApoE$^{-/-}$ mice (Fig. 5*A*). This was due to small (but nonsignificant) reductions in both LDL- and HDL-cholesterol levels in the Nox2$^{-/y}$/ApoE$^{-/-}$ mice (supplemental Fig. 4*A*). Plasma triglyceride levels also appeared to be reduced (by 22%) in 12-wk-old Nox2$^{-/y}$/ApoE$^{-/-}$ mice, but statistical significance was not reached (Fig. 5*B*). There were no differences in total cholesterol and plasma triglycerides between the Nox2$^{-/y}$/ApoE$^{-/-}$ and ApoE$^{-/-}$ strains at 19 wk of age (Fig. 5, *A* and *B*).

Despite these minimal effects on plasma lipid profiles, the en face area of aorta covered by atherosclerotic lesions was ~50% less in Nox2$^{-/y}$ApoE$^{-/-}$ than in ApoE$^{-/-}$ mice at both 12 and 19 wk of age ($P < 0.05$ for both age groups; Fig. 5*C*). Although this study was not designed to analyze lesion burden in individual segments of the aorta, a macroscopic inspection of the arch, thoracic, and abdominal regions appeared to indicate similar reductions in lesion coverage in each anatomical location (supplemental Fig. 5*A*). We also assessed the lesion burden in Nox2$^{-/y}$/ApoE$^{-/-}$ versus ApoE$^{-/-}$ mice by measuring the IMR in cross sections through the aortic sinus. As previously reported (15), there was no difference in IMR in

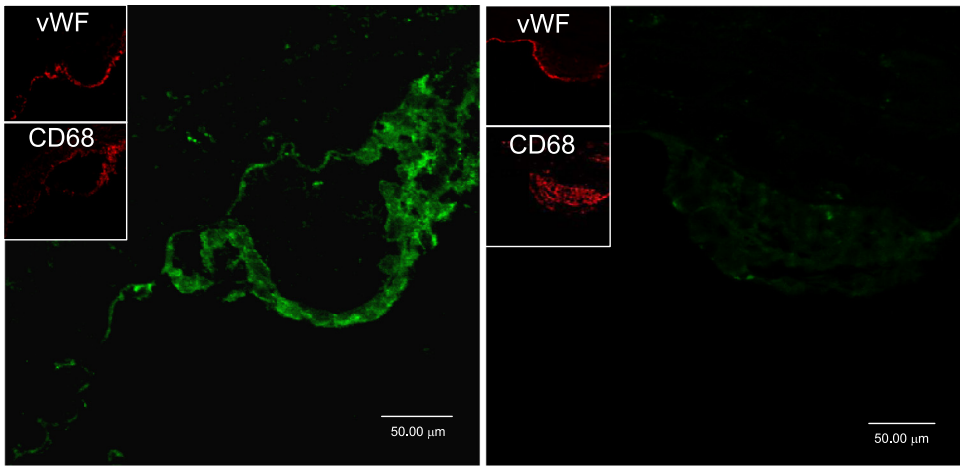

Fig. 4. Absence of Nox2 in aortas from $Nox2^{-/y}/ApoE^{-/-}$ mice. Representative photomicrographs show expression and localization of Nox2 (*inset*: vWF and CD68) in aortas from 19-wk-old $ApoE^{-/-}$ mice maintained on a Western-style diet from 5 wk of age (*left*). By contrast, Nox2 was not detected in aortas from 19-wk-old $Nox2^{-/y}/ApoE^{-/-}$ mice (*right*).

the aortic sinus between the two strains at 12 and 19 wk of age (Fig. 1*D*, and see also supplemental Fig. 5*B*).

Effects of Nox2 Deletion on Superoxide Levels and NO Bioavailability in $ApoE^{-/-}$ Mice

To provide insight into the mechanisms by which the deletion of Nox2 affords protection against plaque development along the aorta of $ApoE^{-/-}$ mice, we compared aortic superoxide levels and NO-dependent vasodilator function between $Nox2^{-/y}/ApoE^{-/-}$ and $ApoE^{-/-}$ mice. Superoxide levels in 12- and 19-wk-old $Nox2^{-/y}/ApoE^{-/-}$ mice were only ~25% of those in age-matched $ApoE^{-/-}$ mice (Fig. 6*A*). By contrast, contractile responses to the NO synthase (NOS) inhibitor L-NAME were markedly higher in $Nox2^{-/y}/ApoE^{-/-}$ mice than in $ApoE^{-/-}$ mice, indicative of improved basal NO bioavailability following Nox2 deletion (Fig. 6*B*). Importantly, contractile responses to U-46619 (0.3 μmol/l) were not different between $ApoE^{-/-}$ (9.7 ± 0.9 mN; $n = 5$) and $Nox2^{-/y}/ApoE^{-/-}$ (10.1 ± 0.4 mN; $n = 7$) mice.

DISCUSSION

The major findings from this study are that *1*) Nox2 expression is upregulated in aortic endothelial cells of $ApoE^{-/-}$ mice before the appearance of atherosclerotic lesions, as well as in

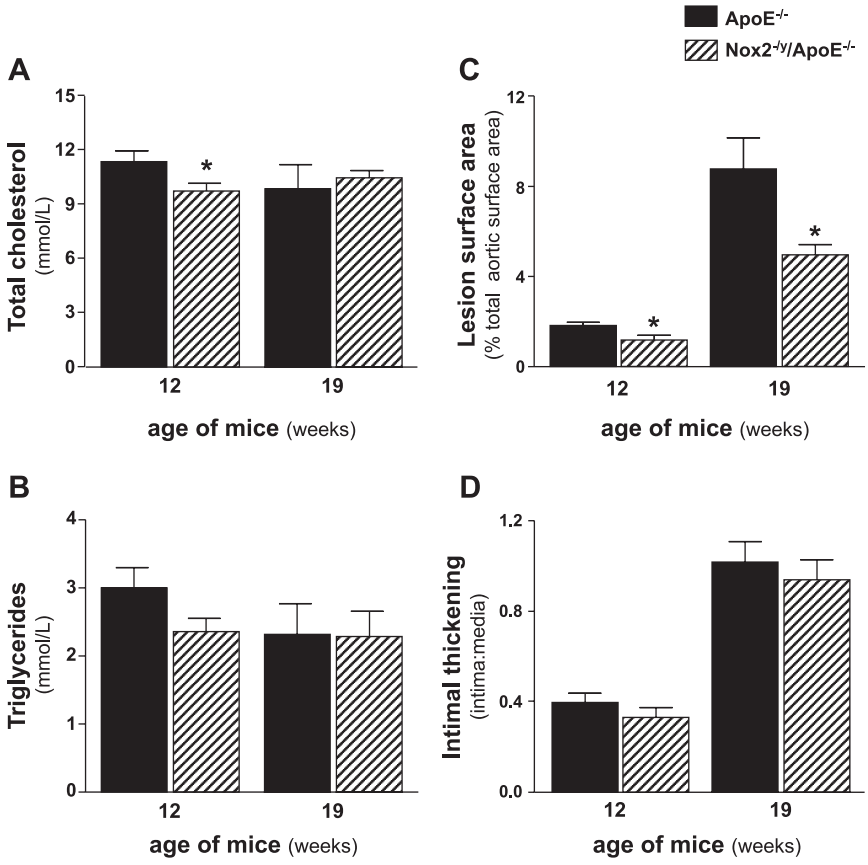

Fig. 5. Absence of Nox2 has minimal effects on plasma lipid profiles but profoundly inhibits plaque development along the aorta in $ApoE^{-/-}$ mice. Total plasma cholesterol (*A*) and triglycerides (*B*) and en face atherosclerotic lesion coverage of the aorta (*C*) and intimal thickening in the aortic sinus (*D*) in $ApoE^{-/-}$ and $Nox2^{-/y}/ApoE^{-/-}$ mice maintained on a Western-style diet from 5 wk of age are shown. *$P < 0.05$ vs. age-matched $ApoE^{-/-}$ mice ($n \geq 5$).

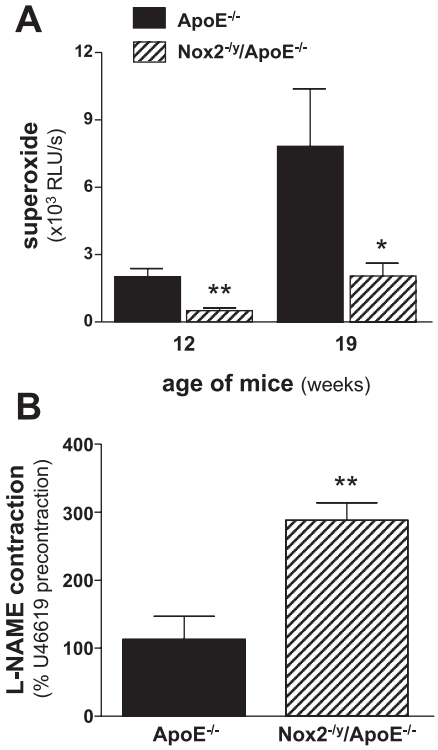

Fig. 6. Reduced superoxide production and augmented nitric oxide bioavailability in aortas from Nox2$^{-/y}$/ApoE$^{-/-}$ vs. ApoE$^{-/-}$ mice maintained on a Western-style diet from 5 wk of age. *A*: reactive oxygen species levels in aortic ring segments from ApoE$^{-/-}$ and Nox2$^{-/y}$/ApoE$^{-/-}$ mice maintained on a Western-style diet from 5 wk of age, measured by L012-enhanced chemiluminescence and expressed as RLU per second per mg of tissue weight. *B*: contractile responses to N^{ω}-nitro-L-arginine methyl ester (L-NAME, 100 μM) in isolated aortic rings from ApoE$^{-/-}$ and Nox2$^{-/y}$/ApoE$^{-/-}$ mice. *$P <$ 0.05 and **$P < 0.01$ vs. age-matched ApoE$^{-/-}$ mice ($n \geq 6$).

macrophages, and these changes are associated temporally with an elevated aortic superoxide production and *2*) the absence of Nox2 (i.e., in Nox2$^{-/y}$/ApoE$^{-/-}$ mice) had minimal impact on plasma lipid profiles but was associated with reduced aortic superoxide production, enhanced NO bioavailability, and marked reductions in atherosclerotic plaque formation along the length of the aorta from arch to iliac bifurcation. These findings thus represent the first definitive evidence of a role for an individual isoform of NADPH oxidase, namely, Nox2, in atherogenesis.

Previous studies comparing disease progression along the aorta of ApoE$^{-/-}$ versus p47$^{phox-/-}$/ApoE$^{-/-}$ double-knockout mice (3, 14, 28) confirmed a cause and effect relationship between NADPH oxidase activity and atherosclerosis. However, these studies provided little insight into the specific roles of individual isoforms of the enzyme since p47^{phox} not only acts as an organizer protein for Nox2-NADPH oxidases but is also likely to be important for vascular Nox1-NADPH oxidase activity (2). Our findings suggest that at least some of the protective effects of p47^{phox} deletion in ApoE$^{-/-}$ mice observed in earlier studies (3, 28) are due to a reduction in Nox2-NADPH oxidase activity. We have shown for the first time that Nox2 protein expression is markedly upregulated in aortas from ApoE$^{-/-}$ mice as young as 12 wk of age. At this age, the lesion burden in the aorta was minimal (i.e., <2%), indicating that Nox2 activity is elevated very early in the disease process. Furthermore, an immunohistochemical analysis of lesion-free aortic sections from ApoE$^{-/-}$ mice suggested that Nox2 expression is elevated before the appearance of lesions, consistent with a causal role for the enzyme in the early activation of critical proatherogenic pathways. Importantly, global deletion of Nox2 in ApoE$^{-/-}$ mice inhibited atherosclerotic lesion development such that the lesion coverage along the length of the aorta in 12- and 19-wk-old Nox2$^{-/y}$/ApoE$^{-/-}$ mice was reduced by ~50% compared with that in age-matched ApoE$^{-/-}$ mice.

In the present study on ApoE$^{-/-}$ mice, as in a previous report on human coronary arteries (26), endothelial cells and macrophages were identified as major sites of Nox2 expression in atherosclerotic plaques. Both of these cell types are also known to express isoforms of the NO-generating family of enzymes known as NOSs. Endothelial cells express a constitutive form of the enzyme called endothelial NOS (eNOS/NOS3), which generates nanomolar levels of NO in response to stimuli such as laminar shear stress across the luminal surface of the endothelium and paracrine factors such as bradykinin and serotonin. Endothelial-derived NO plays a protective role in the vasculature by tonically inhibiting vascular smooth muscle cell contraction and proliferation and by suppressing the adhesion of inflammatory cells and platelets to the endothelium. Thus the absence of eNOS in ApoE$^{-/-}$ mice (i.e., in eNOS$^{-/-}$/ApoE$^{-/-}$ double-knockout mice) was associated with an enhanced atherosclerotic plaque development along the aorta (16). By contrast, macrophages express an inducible isoform of NOS (iNOS/NOS2), which is transcriptionally activated by proinflammatory cytokines and which can generate cytotoxic levels of NO as part of the host defense response. Accordingly, the deletion of iNOS from bone marrow-derived cells, but not parenchymal tissues, in male ApoE$^{-/-}$ mice significantly reduced aortic lesion development (23).

The disregulation of Nox2 activity in cells that express NOS isoforms is likely to be of significance because the direct chemical reaction between the products of these two enzyme systems, namely superoxide and NO, is so fast ($K_m = 1.9 \times 10^9$ $M^{-1} \cdot s^{-1}$) that it is likely to be limited only by diffusion when the two species are present in the same biological compartment (27). Indeed, in the present study we demonstrated that contractions to L-NAME, a nonselective inhibitor of NOS isoforms, were substantially larger in aortic rings from Nox2$^{-/y}$/ApoE$^{-/-}$ mice than in those from ApoE$^{-/-}$mice. Our rationale for acutely inhibiting NOS activity in these vascular reactivity studies was to unmask any tonic NO-mediated relaxation (manifest as a contraction) as a measure of NO bioavailability. Thus the larger contractions to L-NAME in Nox2$^{-/y}$/ApoE$^{-/-}$ mice indicate a higher level of NO bioavailability and provide evidence that Nox2-derived superoxide normally inactivates eNOS- and/or iNOS-derived NO in aortas from ApoE$^{-/-}$ mice.

The inactivation of NO by Nox2-derived superoxide is likely to have dual effects in promoting atherogenesis. First, it will result in a reduction in the bioavailability of vasoprotective endothelium-derived NO, predisposing the vessel wall to vascular inflammation and remodeling. Second, the reaction between superoxide and either eNOS- or iNOS-derived NO will give rise to the powerful oxidizing species peroxynitrite, which is a major mediator of vascular disease via its ability to attack various biomolecules including nucleotides, lipids, and proteins. Furthermore, peroxynitrite

has been shown to oxidize the essential eNOS cofactor tetrahydrobiopterin (BH4) (17). In the absence of BH4, eNOS becomes functionally "uncoupled," i.e., oxygen reduction is uncoupled from L-arginine oxidation such that it switches from an antiatherogenic NO-producing enzyme to one that generates superoxide, thereby itself becoming a contributor to vascular oxidative stress (13). In the present study, we did not directly investigate whether uncoupled eNOS contributed to the elevated levels of ROS detected in aortic rings isolated from 12- and 19-wk-old ApoE$^{-/-}$ mice. However, a previous study using the same mouse model (albeit older animals) showed that the lucigenin-enhanced chemiluminescence signal detected in isolated aortic rings was partially inhibited by acute (i.e., ex vivo) treatment with either L-NAME or the BH4 precursor sepiapterin, suggesting a role for uncoupled NOS in vascular ROS production in ApoE$^{-/-}$ mice (17). When considered in light of this previous study (17), our observation that chronic deficiency of Nox2-NADPH oxidase activity completely prevented the elevation in vascular ROS production in ApoE$^{-/-}$ mice (compare Figs. 1*D* and 4*A*) is consistent with the concept of Nox2-derived ROS acting as an initiating mechanism to beget ROS production by other enzymatic sources, namely, uncoupled eNOS (20).

Although not explored directly in this study, the expression of Nox2 in macrophages may suggest an additional role for this isoform of NADPH oxidase in the formation of oxidized LDL within the blood vessel wall. Oxidized LDL is a major cause of atherosclerotic lesion formation via its ability to enhance cholesterol uptake into macrophages and thereby induce foam cell formation and to activate vascular inflammatory pathways and autoimmune responses. Oxidation of LDL is one of the earliest events in atherogenesis and, as mentioned above, NADPH oxidase activity in macrophages is a critical mediator of this process in mice (24, 28) and humans (6). Given its relatively weak oxidizing potential, it is unlikely that the direct product of NADPH oxidase activity, superoxide, is the major chemical mediator of lipoprotein oxidation by macrophages. Rather, NADPH oxidase-derived superoxide probably contributes to the process by acting either as a cofactor for enzymes that directly cause lipoprotein oxidation (e.g., 15-lipoxygenase) or as a precursor to ROS such as hydrogen peroxide, which are utilized as substrates by enzymes involved in the generation of more powerful oxidizing species such as hypochlorous acid (e.g., myeloperoxidase) (10).

In conclusion, we have provided definitive evidence that Nox2 plays a critical role in elevated superoxide production, reduced NO bioavailability, and atherosclerotic plaque formation in ApoE$^{-/-}$ mice, making this the first study to attribute a proatherogenic function to an individual NADPH oxidase isoform. As such, these studies highlight the Nox2-NADPH oxidase complex as a possible target for future therapies that treat vascular disease by selectively blocking superoxide production at its source. Because of their lack of reliance on outcompeting the diffusion-limited chemical reaction between superoxide and NO and by obviating the formation of downstream ROS and free radicals (e.g., peroxides and tocopheroxyl radicals), such therapies are expected to hold major advantages over conventional antioxidants for ameliorating oxidative stress and endothelial dysfunction in vascular disease.

ACKNOWLEDGMENTS

We acknowledge the technical expertise of Helen Chan (Monash University, Australia) and Angela Coen (Gribbles Pathology, Australia). We are also indebted to Profs. Kathy Griendling and Frank Faraci for valuable comments on the manuscript.

Present address for Anja E. Mast: ZBSA-Zentrum für Biosystemanalyse, Habsburgerstr. 49, 79104, Freiburg, Germany.

GRANTS

This work was supported by National Health and Medical Research Council of Australia Project Grants 300013 and 384163 and Fellowships 465109 (to G. R. Drummond), 350327 (to C. G. Sobey), 400303 (to G. J. Dusting), and 232324 (to S. Selemidis); National Heart Foundation of Australia Grants PF06M2781 (to C. P. Judkins) and PF07M3289 (to B. R. S. Broughton); and a High Blood Pressure Research Council of Australia fellowship (to A. A. Miller).

DISCLOSURES

No conflicts of interest are declared by the author(s).

REFERENCES

1. **Ambasta RK, Kumar P, Griendling KK, Schmidt HH, Busse R, Brandes RP.** Direct interaction of the novel Nox proteins with p22^{phox} is required for the formation of a functionally active NADPH oxidase. *J Biol Chem* 279: 45935–45941, 2004.
2. **Ambasta RK, Schreiber JG, Janiszewski M, Busse R, Brandes RP.** Noxa1 is a central component of the smooth muscle NADPH oxidase in mice. *Free Radic Biol Med* 41: 193–201, 2006.
3. **Barry-Lane PA, Patterson C, van der Merwe M, Hu Z, Holland SM, Yeh ET, Runge MS.** p47^{phox} is required for atherosclerotic lesion progression in ApoE$^{-/-}$ mice. *J Clin Invest* 108: 1513–1522, 2001.
4. **Bedard K, Krause KH.** The NOX family of ROS-generating NADPH oxidases: physiology and pathophysiology. *Physiol Rev* 87: 245–313, 2007.
5. **Bengtsson SH, Gulluyan LM, Dusting GJ, Drummond GR.** Novel isoforms of NADPH oxidase in vascular physiology and pathophysiology. *Clin Exp Pharmacol Physiol* 30: 849–854, 2003.
6. **Bey EA, Cathcart MK.** In vitro knockout of human p47^{phox} blocks superoxide anion production and LDL oxidation by activated human monocytes. *J Lipid Res* 41: 489–495, 2000.
7. **Bjorgvinsdottir H, Zhen L, Dinauer MC.** Cloning of murine gp91^{phox} cDNA and functional expression in a human X-linked chronic granulomatous disease cell line. *Blood* 87: 2005–2010, 1996.
8. **Bleys J, Miller ER 3rd, Pastor-Barriuso R, Appel LJ, Guallar E.** Vitamin-mineral supplementation and the progression of atherosclerosis: a meta-analysis of randomized controlled trials. *Am J Clin Nutr* 84: 880–887, 2006.
9. **Brandes RP, Schröder K.** Composition and functions of vascular nicotinamide adenine dinucleotide phosphate oxidases. *Trends Cardiovasc Med* 18: 15–19, 2008.
10. **Cathcart MK.** Regulation of superoxide anion production by NADPH oxidase in monocytes/macrophages: contributions to atherosclerosis. *Arterioscler Thromb Vasc Biol* 24: 23–28, 2004.
11. **Daiber A, August M, Baldus S, Wendt M, Oelze M, Sydow K, Kleschyov AL, Munzel T.** Measurement of NAD(P)H oxidase-derived superoxide with the luminol analogue L-012. *Free Radic Biol Med* 36: 101–111, 2004.
12. **De Silva TM, Broughton BR, Drummond GR, Sobey CG, Miller AA.** Gender influences cerebral vascular responses to angiotensin II through Nox2-derived reactive oxygen species. *Stroke* 40: 1091–1097, 2009.
13. **Forstermann U, Munzel T.** Endothelial nitric oxide synthase in vascular disease: from marvel to menace. *Circulation* 113: 1708–1714, 2006.
14. **Hsich E, Segal BH, Pagano PJ, Rey FE, Paigen B, Deleonardis J, Hoyt RF, Holland SM, Finkel T.** Vascular effects following homozygous disruption of p47^{phox}: an essential component of NADPH oxidase. *Circulation* 101: 1234–1236, 2000.
15. **Kirk EA, Dinauer MC, Rosen H, Chait A, Heinecke JW, LeBoeuf RC.** Impaired superoxide production due to a deficiency in phagocyte NADPH oxidase fails to inhibit atherosclerosis in mice. *Arterioscler Thromb Vasc Biol* 20: 1529–1535, 2000.
16. **Kuhlencordt PJ, Gyurko R, Han F, Scherrer-Crosbie M, Aretz TH, Hajjar R, Picard MH, Huang PL.** Accelerated atherosclerosis, aortic

aneurysm formation, and ischemic heart disease in apolipoprotein E/endothelial nitric oxide synthase double-knockout mice. *Circulation* 104: 448–454, 2001.

17. **Laursen JB, Somers M, Kurz S, McCann L, Warnholtz A, Freeman BA, Tarpey M, Fukai T, Harrison DG.** Endothelial regulation of vasomotion in ApoE-deficient mice: implications for interactions between peroxynitrite and tetrahydrobiopterin. *Circulation* 103: 1282–1288, 2001.
18. **Martyn KD, Frederick LM, von Loehneysen K, Dinauer MC, Knaus UG.** Functional analysis of Nox4 reveals unique characteristics compared to other NADPH oxidases. *Cell Signal* 18: 69–82, 2006.
19. **Mollnau H, Wendt M, Szocs K, Lassegue B, Schulz E, Oelze M, Li H, Bodenschatz M, August M, Kleschyov AL, Tsilimingas N, Walter U, Forstermann U, Meinertz T, Griendling K, Munzel T.** Effects of angiotensin II infusion on the expression and function of NAD(P)H oxidase and components of nitric oxide/cGMP signaling. *Circ Res* 90: E58–E65, 2002.
20. **Mueller CF, Laude K, McNally JS, Harrison DG.** Redox mechanisms in blood vessels. *Arterioscler Thromb Vasc Biol* 25: 274–278, 2005.
21. **Opitz N, Drummond GR, Selemidis S, Meurer S, Schmidt HH.** The 'A's and 'O's of NADPH oxidase regulation: a commentary on "Subcellular localization and function of alternatively spliced Noxo1 isoforms". *Free Radic Biol Med* 42: 175–179, 2007.
22. **Pollock JD, Williams DA, Gifford MA, Li LL, Du X, Fisherman J, Orkin SH, Doerschuk CM, Dinauer MC.** Mouse model of X-linked chronic granulomatous disease, an inherited defect in phagocyte superoxide production. *Nat Genet* 9: 202–209, 1995.
23. **Ponnuswamy P, Ostermeier E, Schrottle A, Chen J, Huang PL, Ertl G, Nieswandt B, Kuhlencordt PJ.** Oxidative stress and compartment of gene expression determine proatherosclerotic effects of inducible nitric oxide synthase. *Am J Pathol* 174: 2400–2410, 2009.
24. **Rosenblat M, Aviram M.** Oxysterol-induced activation of macrophage NADPH-oxidase enhances cell-mediated oxidation of LDL in the atherosclerotic apolipoprotein E deficient mouse: inhibitory role for vitamin E. *Atherosclerosis* 160: 69–80, 2002.
25. **Selemidis S, Sobey CG, Wingler K, Schmidt HH, Drummond GR.** NADPH oxidases in the vasculature: molecular features, roles in disease and pharmacological inhibition. *Pharmacol Ther* 120: 254–291, 2008.
26. **Sorescu D, Weiss D, Lassegue B, Clempus RE, Szocs K, Sorescu GP, Valppu L, Quinn MT, Lambeth JD, Vega JD, Taylor WR, Griendling KK.** Superoxide production and expression of nox family proteins in human atherosclerosis. *Circulation* 105: 1429–1435, 2002.
27. **Thomas SR, Witting PK, Drummond GR.** Redox control of endothelial function and dysfunction: molecular mechanisms and therapeutic opportunities. *Antioxid Redox Signal* 10: 1713–1766, 2008.
28. **Vendrov AE, Hakim ZS, Madamanchi NR, Rojas M, Madamanchi C, Runge MS.** Atherosclerosis is attenuated by limiting superoxide generation in both macrophages and vessel wall cells. *Arterioscler Thromb Vasc Biol* 27: 2714–2721, 2007.
29. **Wendt MC, Daiber A, Kleschyov AL, Mulsch A, Sydow K, Schulz E, Chen K, Keaney JF Jr, Lassegue B, Walter U, Griendling KK, Munzel T.** Differential effects of diabetes on the expression of the gp91^{phox} homologues nox1 and nox4. *Free Radic Biol Med* 39: 381–391, 2005.